

Protic Ionic Liquid as an Alternative Electrolyte for Simultaneous Electrochemical Determination of Caffeine and Nicotine in Environmental and Food Samples

José Fernando de Macedo,^{1b}*^a Jonatas O. S. Silva,^{1b}^a José Felipe dos Santos,^{1b}^a
José Carlos dos Santos Júnior,^{1b}^a Micael S. Matos^{1b}^a and Eliana M. Sussuchi^{1b}^a

^aGrupo de Pesquisa em Sensores Eletroquímicos e nano(Materiais) (SEnM),
Laboratório de Corrosão e Nanotecnologia (LCNT), Programa de Pós-Graduação em Química,
Departamento de Química, Universidade Federal de Sergipe (UFS), 49107-230 São Cristóvão-SE, Brazil

Caffeine (CAF) and nicotine (NIC) are emerging contaminants and are among the most consumed substances in the world, making it crucial to monitor these contaminants. In this work, an alternative electrolyte, 2-hydroxyethylammonium acetate (2HEAA) was used for the development of an electroanalytical method for determination and quantification of CAF and NIC, simultaneously, using differential pulse voltammetry (DPV). The system with the 2HEAA electrolyte was characterized by cyclic voltammetry and electrochemical impedance spectroscopy, and the DPV parameters were optimized for the best conditions. The method was validated from a calibration curve obtained which showed limit of detection (LOD) of 0.82 and 6.26 $\mu\text{mol L}^{-1}$ and limit of quantification (LOQ) of 2.73 and 20.8 $\mu\text{mol L}^{-1}$ for CAF and NIC, respectively. In the precision analyses, values lower than 10% of relative standard deviation were obtained. In the presence of concomitant inorganic and organic species, the system proved to be selective in the determination of analytes. The method was used to determine the analytes in fortified samples (river water, synthetic urine and commercial milk), obtaining recoveries between 87.25 and 111.40%. The 2HEAA demonstrated high efficiency as an alternative electrolyte with good signal-to-noise ratio, increased analytical sensitivity of the method, in addition to presenting low cost and fast electrolyte preparation.

Keywords: alkaloids, monitoring, emerging contaminants, 2-hydroxyethylammonium acetate, green chemistry

Introduction

Nicotine (NIC) and caffeine (CAF) belong to the class of alkaloids and are among the most widely consumed nervous system stimulants in worldwide. NIC consumption accounts for 20% of the population of the world, with approximately six trillion cigarettes consumed globally, of which approximately four and a half trillion are improperly disposed of in the environment.¹ Regarding CAF, in the years of 2021 and 2022, approximately 1.06×10^7 tons of coffee were consumed worldwide, underscoring its popularity and significant presence in the diet and culture of diverse societies.^{2,3} Improper disposal of products containing these substances has become problematic due to their accumulation in the environment.

Nicotine (3-[(2S)-1-methyl-2-pyrrolidinyl]pyridine) is naturally occurring in tobacco plants and is predominantly consumed through conventional and electronic cigarettes, which are the main sources of bioavailability.¹ Caffeine (1,3,7-trimethyl-3,7-dihydro-1H-purine-2,6-dione) is primarily obtained from coffee, one of the most globally consumed beverages, and is also present in beverages such as soft drinks and energy drinks.^{2,3} The stimulation induced by NIC and CAF results in sensations of pleasure, acting on various mechanisms in the human body.^{4,5}

In contrast, pathologies associated with nicotine exposure encompass malignant neoplasms, including lung carcinoma, larynx, esophagus, and bladder cancers, as well as obstructive respiratory disorders, such as chronic bronchitis and pulmonary emphysema.^{3,6} Excessive caffeine consumption can lead to variety of adverse side effects, including anxiety, restlessness and nervousness, irritability, diarrhea, muscle tremors and irregularities in heartbeat, and complications in the development of fetuses.⁷⁻⁹ Based on

*e-mail: macedojf92@gmail.com

Editor handled this article: Rodrigo A. A. Muñoz (Associate)



this, the European Food Safety Authority had set a dose of 400.0 mg (about 5.7 mg kg⁻¹) for daily CAF consumption¹⁰ and is established 0.3 mg kg⁻¹ maximum residue limit for NIC.¹¹

The environmental risks associated with cigarettes and the potential NIC contamination are imminent. Factors such as NIC's high solubility in water, low vapor pressure, and the significant amount of discarded cigarette butts contribute to the contamination of aquatic ecosystems.¹²⁻¹⁴ CAF enters water bodies through sewage system, exerting a substantial impact on water quality and aquatic biodiversity. Although coffee grounds are commonly employed as a soil fertilizer, the presence of CAF can hinder plant development.¹⁵

Voltammetric techniques are commonly utilized for monitoring contaminating species due to their low cost, ease of operation, and high sensitivity. Electrochemical sensors modified with various materials (biochar, nanomaterials, and others) are often the focus point of research in electroanalysis.^{16,17} Conversely, the supporting electrolyte plays a crucial role as the medium in which redox processes occur, directly influencing the composition of the solution-electrode interface.

Ionic liquids (ILs) have been increasingly explored in the field of electrochemistry with particular attention given to protic ILs. There are reports of ILs being utilized as modifiers of sensors,¹⁸ biosensors,¹⁹ and as electrolytes for batteries,²⁰ supercapacitors,²¹ and in the electro-reduction of CO₂.²² Ionic liquids are organic salts with a melting point below 100 °C, consisting of an organic cation and an organic or inorganic anion. Through the combination of different ions, the properties of ILs are adjustable, providing these compounds with high thermal and electrochemical stability, a wide potential window, negligible volatility and excellent conductivity. The diverse properties of ILs can enhance electrolyte safety and contribute to the advancement of this technology.²⁰

The function of the supporting electrolyte is to confine potential differences to a narrow region close to the electrode, to reduce analyte migration and solution resistance.²³ Some of the criteria for a substance to be considered as a supporting electrolyte is to be inert and have a wide range of measurable potentials. Ionic liquids meet these requirements and, therefore, investigating them in electroanalytical processes, as occurs for energy storage,^{20,21,24} will allow exploring the wide potential window that these compounds present and which is limited in conventional electrolytes. Thus, electroactive species with high oxidation and/or reduction potentials can be investigated by voltammetric techniques.

The application of ILs as electrolytes primarily

aims to enhance the performance of batteries and supercapacitors.^{20,21} The assessment of ILs as electrolytes in supercapacitors primarily focuses on properties such as ionic conductivity, viscosity, and ion size.²¹ In electrochemical analyses, interfacial processes play a crucial role in facilitating reactions on the electrode surface, and the function of the electrolyte is to reduce the resistance to charge transfer within the system.²³ To date, no reports have been found of the application of ILs as supporting electrolyte in the determination of contaminant species through electroanalytical methods.

Therefore, this study aimed to develop a voltammetric method utilizing 2-hydroxyethylammonium acetate (2HEAA) as a supporting electrolyte to enhance the electrochemical signal. This approach enables sensitive, selective and simultaneous determination of nicotine and CAF in samples of river water, synthetic urine and milk.

Experimental

Reagents and solutions

Caffeine (C₈H₁₀N₄O₂, 99.0%) and nicotine (C₁₀H₁₄N₂, 99.0%) were purchased from Sigma-Aldrich (St. Louis, United States). Sodium hydroxide (NaOH, 98.0%) and potassium chloride (KCl, 99.5%) were acquired from Dinâmica (Indiatuba, Brazil). Dibasic sodium phosphate (Na₂HPO₄, 99.0%), monobasic sodium phosphate (NaH₂PO₄, 99.0%), potassium ferricyanide K₃[Fe(CN)₆], 99.5%) and potassium ferrocyanide trihydrate (K₄[Fe(CN)₆].3H₂O, 99.0%) were obtained from NEON (São Paulo, Brazil). All solutions were prepared by diluting the standards in ultrapure water obtained from the Millipore Milli-Q system with a resistivity 18.2 MΩ cm. Stock solutions of caffeine (1.50 mmol L⁻¹) and nicotine (19.6 mmol L⁻¹) were prepared in ultrapure water. Aliquots were added to the electrochemical cell for analyzes.

For the preparation of the alternative electrolyte (2HEAA) stock solution (0.50 mol L⁻¹), 3.03 g of 2HEAA viscous liquid was diluted in ultrapure water with a final volume of 0.05 L and stored at 22 °C in a glass bottle. Aliquots of this solution were utilized to obtain 10.0 mL of dilute solution (0.05 mol L⁻¹), which was added to the electrochemical cell for analysis. The KCl supporting electrolyte solution was prepared at a concentration of 1.00 mol L⁻¹ and used on the same day of measurements. The phosphate buffer solution was prepared by adding 0.0056 mol L⁻¹ of HPO₄²⁻, 0.0033 mol L⁻¹ of H₂PO₄⁻ and 1.0500 g of sodium chloride with a final volume of 0.05 L. The pH was adjusted to 7.0 using a 3.00 mol L⁻¹ NaOH solution.

Synthesis and characterization of 2-hydroxyethylammonium acetate

The protic ionic liquid (PIL) was synthesized in an equimolar ratio 1:1.²⁵ A methanolic solution of 2-aminoethanol was added to the flask with vigorous stirring, followed by the slow addition of the acetic acid. The mixture was kept under reflux and constant stirring at 22 °C for 2 h. Methanol was then removed under reduced pressure at a temperature of 50 °C. The resulting PIL was stored in a desiccator at room temperature in the presence of silica to humidity control. A summary of its properties can be seen in Table 1. Structural characterization information (Table S1) and the investigated properties of 2HEAA are presented in Figure S1 (Supplementary Information (SI) section).

Electrochemical analysis

The electrochemical experiments were conducted using an Autolab PGSTAT 100N Potentiostat/Galvanostat model controlled by the NOVA 2.1.6 software for monitoring and data treatment. A three-electrode system and an electrochemical cell with a capacity of 15.0 mL were used in this study. A glassy carbon electrode (GCE) served as the working electrode (diameter (\varnothing) = 3.00 mm), platinum wire (\varnothing = 2.00 mm) was used as an auxiliary electrode, and the reference electrode composed of Ag/AgCl in KCl solution (3.00 mol L⁻¹). The GCE was cleaned by sonication with acetone and ethanol for 5 min. Before each measurement, the GCE was polished in alumina suspension (1.0 μ m) with the support of a polishing cloth to renew the surface. The electrochemical behavior of the systems was investigated using cyclic voltammetry (CV) and electrochemical impedance spectroscopy (EIS) in the presence of 1.00 mmol L⁻¹ of the redox probe [Fe(CN)₆]^{3-/4-} with KCl (1.00 mol L⁻¹) as the standard electrolyte compared to 2HEAA (0.05 mol L⁻¹) as an alternative electrolyte. A similar study was carried out for NIC (32.0 mmol L⁻¹) and CAF (2.99 mmol L⁻¹), comparing the electrochemical behaviors of the species in phosphate buffer (pH 7.0) with the electrolyte 2HEAA (0.05 mol L⁻¹, pH 6.3), varying the scan rate from 100 to 500 mV s⁻¹.

Differential pulse voltammetry (DPV) was employed to establish the analytical method. The 2HEAA solution (0.05 mol L⁻¹) containing 15.0 and 196 μ mol L⁻¹ of CAF

and NIC, respectively, was subjected to different pH (4.3 to 8.3) and preconcentration time (0 to 90 s) conditions to determine the optimal parameters. The pH of the supporting electrolyte was adjusted with 1.00 mol L⁻¹ solutions of HCl or NaOH to achieve pH values of 4.3, 5.3, 7.3 and 8.3. DPV conditions, including scan rate, modulation time, and modulation amplitude were optimized, and the results can be found in the SI section (Figure S4).

Calibration curves were obtained by simultaneous and consecutive additions of the analytes at concentrations ranging from 4.97 to 34.42 μ mol L⁻¹ for CAF and 21.89 to 393.7 μ mol L⁻¹ for nicotine. Measurements were conducted in triplicate (n = 3) and standard deviations were calculated. The limits of detection (LOD) and quantification (LOQ) were determined considering the standard deviation (S_d) obtained from 10 measurements performed on the supporting electrolyte (“blank”). The calibration curve was established by correlating the current at the anodic peak with the analyte concentration. The equations used were: LOD = 3 (S_d/b) and LOQ = 10 (S_d/b) where b represents the slope of the linear regression.

Precision (repeatability and reproducibility) and selectivity tests were performed in the presence of 3.05 μ mol L⁻¹ CAF and 138.3 μ mol L⁻¹ NIC in 2HEAA solution (0.05 mol L⁻¹) (pH 6.3). Repeatability was evaluated by conducting five measurements using a single 2HEAA solution, while reproducibility was assessed by performing measurements in five different 2HEAA solutions. To assess selectivity, both inorganic (CaCl₂, NaCl, KCl, NH₄Cl, MgCl₂, and Na₂SO₄) and organic (urea, ascorbic acid, sucrose, and glucose) species were investigated as possible interferers in the signal-response of the analytes. Measurements were carried out with both analytes present in the electrochemical cell, obtaining two levels of concentrations. CAF was evaluated at 1.0:1.0 (level 1) and 1.0:45.0 (level 2) ratios, and nicotine was evaluated at 1.0:1.0 (level 1) and 1.0:0.02 (level 2) ratios. The difference in the ratio of the analytes at level 2 is due to the difference in the linear range of CAF and NIC concentrations.

Obtaining and determining analytes in river water, synthetic urine and commercial milk

The synthetic urine solution was prepared following the methodology described by Silva *et al.*¹⁶ The milk sample

Table 1. Properties of 2-hydroxyethylammonium acetate (2HEAA)

PIL	Toxicity / (mmol L ⁻¹)	Td / °C	η / (mPa s ⁻¹)	σ / (mS cm ⁻¹)	EPW / V
2HEAA	16.14	169.0	885.3	3.117	5.56

PIL: protic ionic liquid; Td: decomposition temperature; η : viscosity, σ : conductivity at 0.05 mol L⁻¹; EPW: electrochemical potential window.

was purchased from local shops. The river water sample was obtained from a farmer in the municipality of Tobias Barreto, Sergipe, Brazil (11°08'46.7"S 37°49'52.4"W).

Samples of river water and synthetic urine were filtered using a 0.45 μm membrane prior to the addition of analytes. For the analyses, aliquots of 50.0 μL of the fortified samples were added to the electrochemical cells containing 10.0 mL of the electrolyte (2HEAA 0.05 mol L⁻¹, pH 6.3). For the milk sample, 50.0 μL were diluted in 5.00 mL of the electrolyte to decrease the matrix effect on the electrochemical signal of the analytes.

The accuracy of the method was assessed by determining the recovery of the analytes in the fortified samples. Known concentrations of the analytes were added to the samples

and recovery curves were constructed. The obtained values were expressed as a percentage of recovery, calculated using the following equation: $\text{recovery (\%)} = (C_{\text{rec}}/C_{\text{add}}) \times 100$, where C_{rec} corresponds to the concentration obtained by the method and C_{add} represents the added analyte concentration.

Results and Discussion

Electrochemical characterization of electrolytes

The electrochemical characterizations of the systems were conducted using a GCE via cyclic voltammetry (Figure 1), wherein variations in the scan rate (25-300 mV s⁻¹) were examined. The systems comprised 1.00 mmol L⁻¹ of

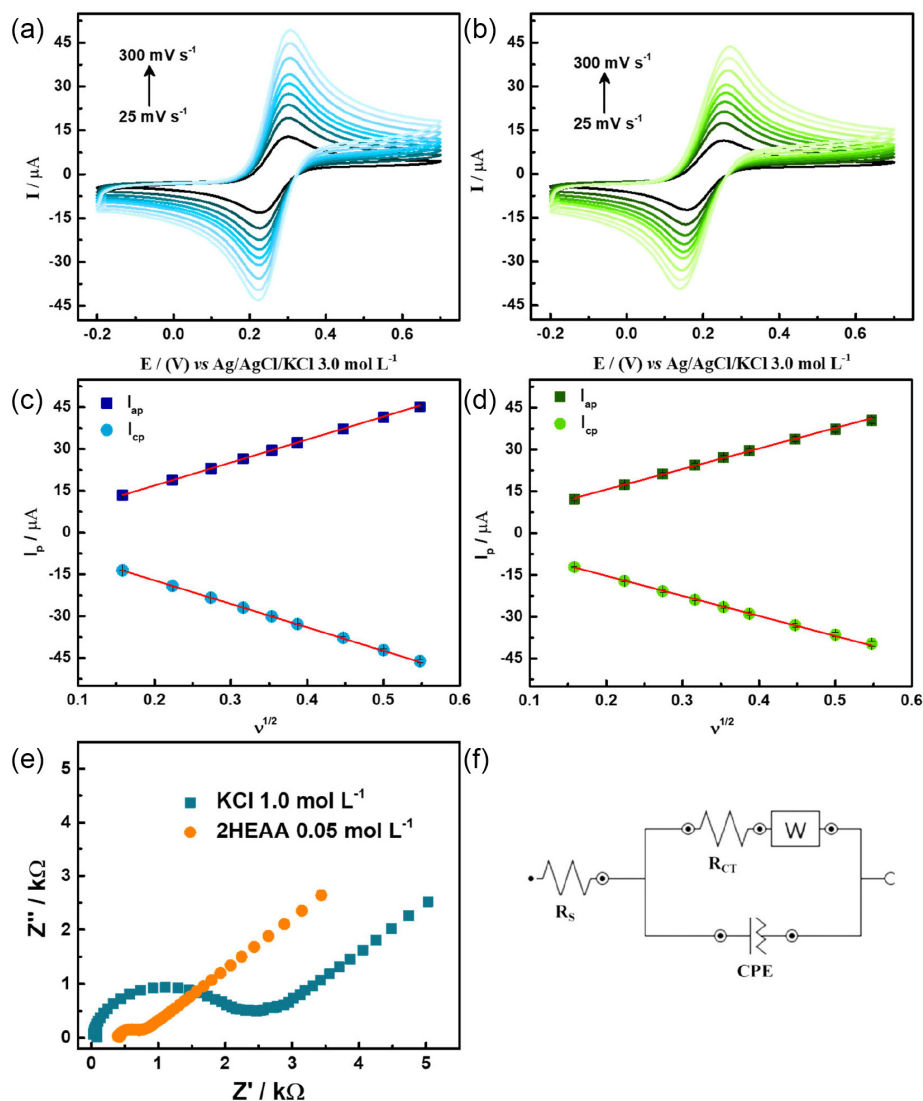


Figure 1. (a) CV obtained for 1.00 mmol L⁻¹ of [Fe(CN)₆]^{3-/4-} using GCE in a solution of 1.00 mol L⁻¹ of KCl; (b) 0.05 mol L⁻¹ of 2HEAA (pH 6.3) employing different scan rate (25.0-300 mV s⁻¹). Graphs depicting the variation of the current intensities of the anodic (I_{ap}) and cathodic (I_{cp}) peaks as a function of the square root of the scan rate ($v^{1/2}$), obtained in a solution of (c) 1.00 mol L⁻¹ of KCl; and (d) 0.05 mol L⁻¹ of 2HEAA; (e) Nyquist diagrams obtained using GCE in the presence of 1.00 mmol L⁻¹ of [Fe(CN)₆]^{3-/4-} in solution 1.00 mol L⁻¹ of KCl and 0.05 mol L⁻¹ of 2HEAA, under a frequency range of 100 kHz to 0.1 Hz and amplitude of 10 mV; (f) representation of an equivalent circuit similar to the Randles circuit.

the redox probe $[\text{Fe}(\text{CN})_6]^{3-/4-}$ in the presence of a KCl solution (1.00 mol L^{-1}) for the supporting electrolyte, referred as conventional (Figure 1a), and 2HEAA ionic liquid (0.05 mol L^{-1}) for the alternative electrolyte (Figure 1b). Graphs were generated by correlating the current intensities of the anodic (I_{ap}) and cathodic (I_{cp}) peaks with the square root of the scan rate ($v^{1/2}$) (Figures 1c and 1d). The obtained results indicate the similarity between the voltammetric behaviors of the evaluated systems. In both cases, linearity between the variations observed in I_{ap} and I_{cp} as a function of $v^{1/2}$ is evident, with linear correlation coefficients (R^2) equal to 0.998 and 0.999, respectively, in the presence of 2HEAA, and equal to 0.999 for both I_{ap} and I_{cp} in KCl solution. Thus, based on the Randles-Ševčík equation, the charge transfer process in both systems is diffusion-controlled. Additionally, the observed variations in the peak potentials (ΔE_p) and peak ratios ($I_{\text{ap}}/I_{\text{cp}}$) support the characterization of the systems as *quasi-reversible*.^{18,26}

The systems were further characterized by electrochemical impedance spectroscopy (EIS) and the results are depicted in Figures 1e-1f. By fitting the semicircles obtained in the Nyquist plots, using the inserted circuit, the charge transfer resistance (R_{CT}) value of the GCE in the presence of the different electrolytes containing the redox probe $[\text{Fe}(\text{CN})_6]^{3-/4-}$ was determined. The variation of the system value in the R_{CT} when using different supporting electrolytes is evident, being equal to 312Ω and 2100Ω , to 2HEAA and KCl, respectively.

This indicates an approximately seven-fold reduction in R_{CT} when 2HEAA was employed, suggesting that the utilization of 2HEAA as a supporting electrolyte enhances the charge transfer process, likely due to the presence of ionic liquid-forming ions. Similar behavior was observed in a study investigating three hydroxyethylammonium-based ILs.²¹ The results indicated that supercapacitors with IL-based electrolytes exhibited superior performance compared to the conventional system, and the IL with lower anion and viscosity, along with higher conductivity and lower resistance to charge transfer, demonstrated the best performance.

Study of the voltammetric behavior of analytes in the presence of 2HEAA

In this study, 2HEAA (0.05 mol L^{-1}) served as a supporting electrolyte for the simultaneous investigation of the voltammetric behavior of NIC and CAF. Cyclic voltammetry was employed, with variations in the scan rate ranging from 100 and 500 mV s^{-1} . Analysis of the voltammograms depicted in Figures 2a-2b facilitated the evaluation of the electrochemical behavior of the analytes. Notably, the absence of reduction peaks in the evaluated potential ranges suggests that the oxidation process is irreversible for both analytes.^{27,28} Furthermore, the graphs presented in Figure 2c, utilizing the Randles-Ševčík equation, indicate that the charge transfer process of

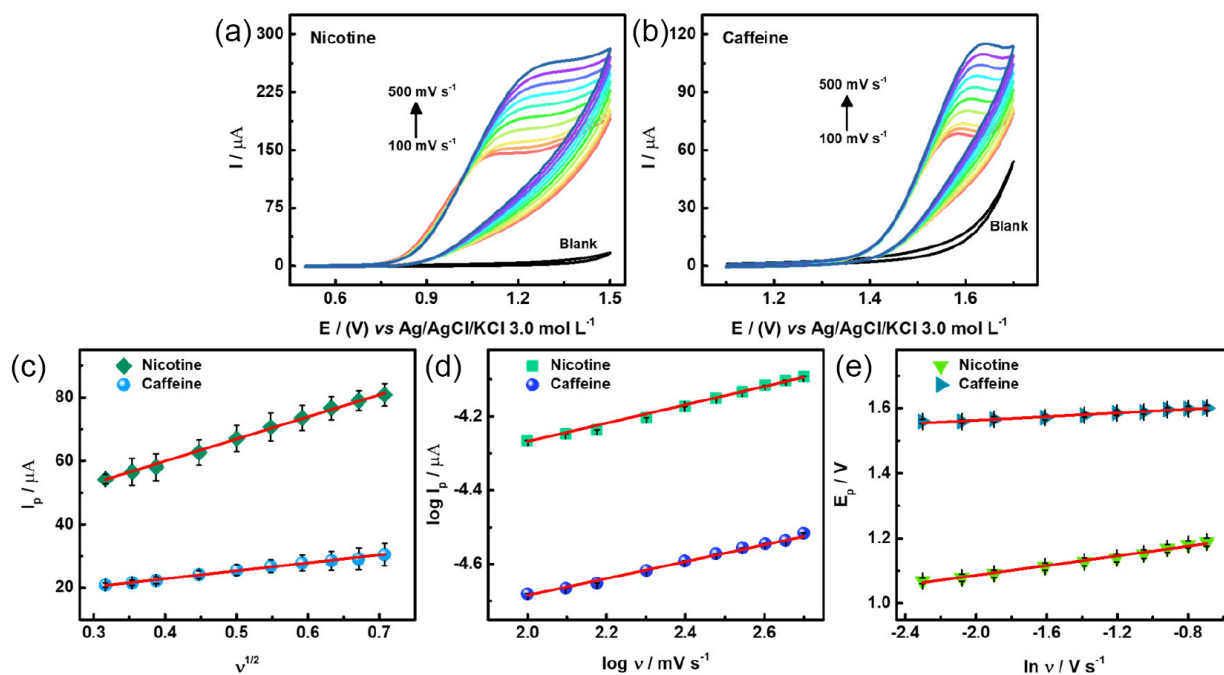


Figure 2. CV obtained using a GCE in 2HEAA solution (0.05 mol L^{-1} , pH 6.3) in the presence of (a) nicotine (32.0 mmol L^{-1}) and (b) caffeine (2.99 mmol L^{-1}) employing different scan rate between 100 and 500 mV s^{-1} ; (c) graphs of the variation of I_p versus $v^{1/2}$; (d) dependence of the logarithm of I_p as a function of the logarithm of the scan rate (v); (e) graphs of the variation of E_p versus $\ln v$.

the analytes occurs via diffusion, as evidenced by the linearity.^{18,26} Figure 2d illustrates the linear correlation between the logarithm of the analyte current intensity and the logarithm of the scan rate, exhibiting slopes of 0.26 ($R^2 = 0.994$) and 0.24 ($R^2 = 0.995$) for NIC and CAF, respectively. This linear relationship allows for the identification of the type of interfacial process taking place, based on the slope value. Specifically, a coefficient value of 1.00 suggests the occurrence of an adsorptive process, whereas a value of 0.50 supports a diffusional process.^{26,28} In this instance, the obtained angular coefficients less than 0.50 indicate that the charge transfer between the electrode and analytes occurs within the diffuse layer region.

From the E_p vs. $\ln v$ relationship presented in Figure 2e, it is possible to estimate the amount of electron transferred during the oxidation process of NIC and CAF. Considering that the process is controlled by diffusion, it can be assumed that $\alpha = 0.5$. Applying the slope value of E_p vs. $\ln v$ in the simplified Laviron's equation¹⁸ (slope = $RT/\alpha nF$), using 2HEAA (0.05 mol L⁻¹, pH 6.3) as electrolyte, where R is the gas constant (8.314 J mol⁻¹ K⁻¹), T is the temperature in Kelvin (298.15 K), F is the Faraday constant (96,480 C), $\alpha = 0.5$ for irreversible process. The electron number values obtained were 0.66 ($R^2 = 0.99$) and 1.82 ($R^2 = 0.98$) for NIC

and CAF, respectively. Similar electron number values were obtained for phosphate buffer (pH 7.0), 1.25 ($R^2 = 0.99$) for NIC and 2.42 ($R^2 = 0.99$) for CAF. The electrochemical behavior in phosphate buffer (PBS) is available in the SI section (Figure S2 and Table S2).

The electron numbers estimated indicates that CAF oxidation occurs with the transfer of 2 electrons, corroborating other studies.^{28,29} For NIC, the electron numbers are different from other studies,³⁰⁻³² indicating that for systems with 2HEAA and PBS electrolytes using commercial GCE, nicotine electrooxidation follows different mechanisms.

A comparative analysis between 2HEAA and conventional electrolytes were carried out using cyclic voltammetry. The blanks show lower background current in 2HEAA compared to those obtained in PBS (Figures 3a-3b). CVs obtained for CAF and NIC (Figures 3c-3d) show better peak definition in the alternative electrolyte (2HEAA) with a width at half peak height ($W_{1/2}$) of 0.25 V (2HEAA) and 0.32 V (PBS) for nicotine and 0.12 V (2HEAA) and 0.10 V (PBS) for caffeine resulting in greater selectivity when using 2HEAA. Furthermore, shifts in the anodic peak of the analytes to less positive values were observed in the presence of 2HEAA, which indicates a lower energy expenditure during the reaction. In

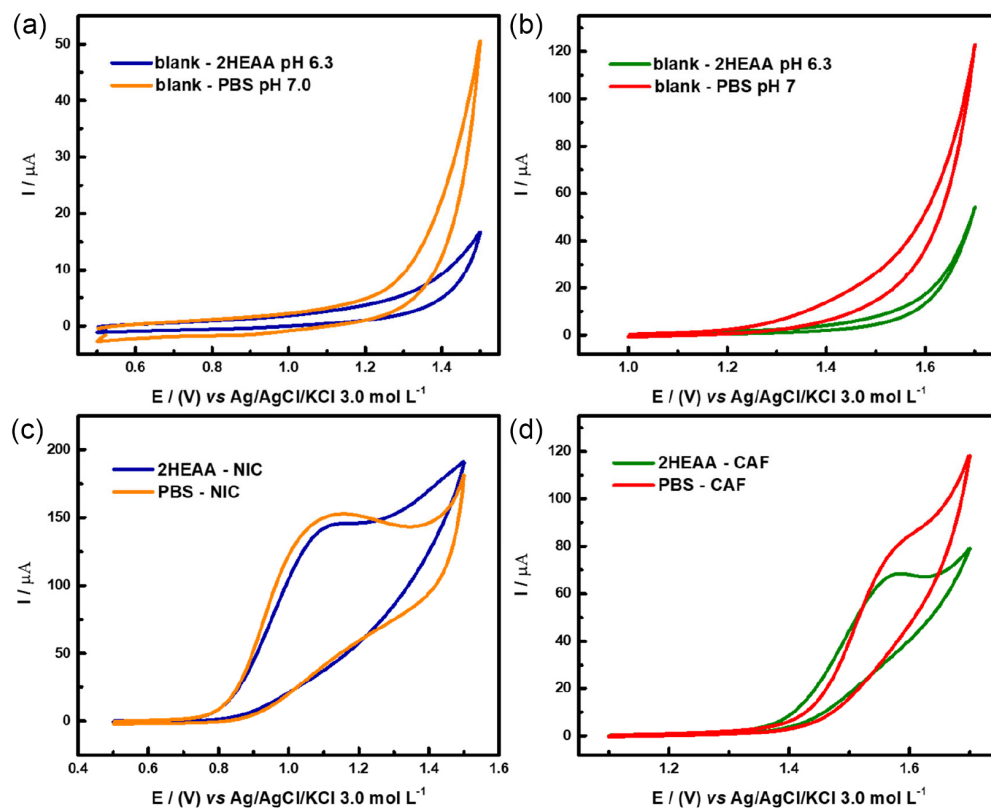


Figure 3. CV obtained with 2HEAA and PBS electrolytes in the absence of analytes (blank) in the oxidation potential range of (a) nicotine and (b) caffeine. CV obtained for (c) nicotine 32.0 mmol L⁻¹ and (d) caffeine 2.99 mmol L⁻¹ in electrolytes 2HEAA and PBS at 100 mV s⁻¹.

addition, 2HEAA ensures a lower charge transfer resistance as discussed in Figure 1e.

Optimization of analysis parameters

The supporting electrolyte plays a crucial role in establishing the concentration gradient that counteracts the repulsive forces on the surface of the electrode, leading to the formation of the electrical double layer (interface).³³ This interface represents the region of electrical neutrality where the molecules of the electrolyte solution are immobilized and adsorbed onto the surface of the electrode, forming the internal layer. Nevertheless, the external or diffuse layer constitutes the region where the solvated analytes are present, exhibiting higher mobility and being attracted to the electrode due to long-range interactions generated.^{26,34} Consequently, the supporting electrolyte directs the analytes toward the diffuse layer, highlighting its significance in creating a stable electric double layer to facilitate interfacial processes. Therefore, the concentration of the electrolyte is crucial for establishing an appropriate concentration gradient to support the formation of a stable electrical double layer, ensuring the occurrence of interfacial processes. Figure 4 depicts the results of the study evaluating the effect of IL 2-hydroxyethylammonium acetate concentration on the determination of CAF and NIC using DPV.

The data presented in Figure 4a illustrate the current intensities of the analytes evaluated separately as a function of different concentrations of the alternative electrolyte. These findings suggest that a concentration of 0.05 mol L⁻¹ of 2HEAA promotes the oxidation of CAF, whereas for NIC, the difference in current intensity between concentrations of 0.05 and 0.10 mol L⁻¹ is considerably small. In Figure 4b, the analyses conducted for the simultaneous determination of the analytes at two

concentrations of the supporting electrolyte (0.05 and 0.01 mol L⁻¹) indicate that the I_p of NIC doubled in intensity compared to that observed in the individual analysis. The varying concentrations of 2HEAA evaluated influence the diffuse layer, resulting in two extreme conditions. The higher concentration (0.20 mol L⁻¹) impedes the diffusion process, partially hindering the diffusion of the analytes (Figure 4a) on the electrode surface. Conversely, at the lowest concentration (0.01 mol L⁻¹), the analytes are not efficiently directed to the electrode surface. This behavior was observed in a study that evaluated different concentrations of various supporting electrolytes.²³ The voltammetric responses at different concentrations of the 2HEAA supporting electrolyte suggest that the optimal concentration for the oxidation processes of the analytes is 0.05 mol L⁻¹.

To assess the influence of supporting electrolyte pH and preconcentration time on the oxidation reaction of CAF and NIC (Figures 5a-5d), the 0.05 mol L⁻¹ solution of 2HEAA had its pH adjusted to values between 4.3-8.3. Subsequently, the pre-concentration time (0 to 90 s) was investigated, with measurements performed in the presence of 196.0 μmol L⁻¹ of nicotine and 15.0 μmol L⁻¹ of CAF. The results reveal a gradual increase in NIC and CAF signals with the rise in the pH of the supporting electrolyte. However, upon comparing the signals obtained for the electrolyte in the absence of analytes, an oxidation peak ca. +1.4 V (E vs. Ag/AgCl) emerges in the CAF oxidation region (Figures S3b-S3f, SI section), contributing to increased intensity with pH elevation. This phenomenon is associated with the oxidation of the anion of the ionic liquid, 2-hydroxyethylammonium acetate, which in the basic medium has available electrons to donate to the reaction. Another factor is the presence of OH⁻ radicals generated on the carbon electrodes surface, which may be influencing the oxidation peak observed at pH 6.3, 7.3 and 8.3.³⁵ Conversely,

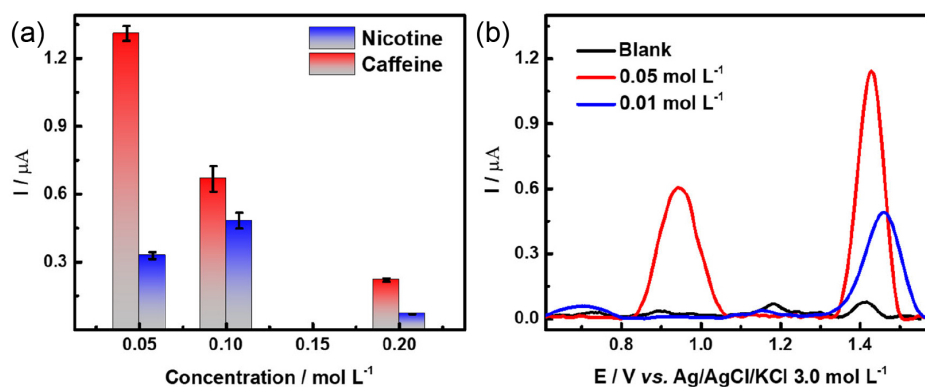


Figure 4. Data obtained using GCE in the presence of CAF (30.0 μmol L⁻¹) and NIC (196.0 μmol L⁻¹) at different concentrations of 2HEAA. (a) Graph of the relationship between the current intensities obtained in the analyses of the analytes individually and the concentrations of the 2HEAA electrolyte used (0.05 mol L⁻¹, pH 6.3; 0.10 mol L⁻¹, pH 6.4 and 0.20 mol L⁻¹, pH 6.5); (b) differential pulse voltammograms obtained under different concentrations of the 2HEAA electrolyte (0.05 and 0.01 mol L⁻¹, pH 6.2).

in acidic media, this reaction is hindered due to the presence of H^+ ions. Hence, the optimal signal-to-noise ratio was achieved at pH 6.3, with CAF current intensity being approximately 13 times higher than “blank” noise, while no additional electrooxidation peak was observed in the NIC oxidation potential region (Figure S3d).

In Figures 4b-4c, a nonlinear behavior is observed between the E_p values of NIC and CAF with the variation of the pH of the 2HEAA solution. The oxidation potential of CAF remains practically unchanged with the increase of pH, a behavior observed in other systems that utilized PBS³⁶ and Britton-Robinson buffer (B-R) solutions.²⁸ In another work²⁹ using PBS, a linear relationship between E_p and pH was observed for CAF and NIC, suggesting that this relationship between the pH of the supporting electrolyte and E_p is more dependent on the type of interaction on the surface of the working electrode. Therefore, the mechanism of electrooxidation of CAF and NIC may follow different paths on different surfaces of the electrodes.²⁸ Consequently, it was not feasible to evaluate the ratio between the number of electrons and protons transferred during the oxidation reaction of the analytes, as reported in other studies.^{27,29} However, parameters as the lowest R_{CT} of 2HEAA observed in Figure 1f and the diffusion-controlled processes for NIC and CAF in Figure 2c indicate that 2HEAA improves the performance of the diffuse layer, which intermediate in reactions through the “active” (mobile) proton of PIL.²⁰

The pre-concentration time study (Figure 5d) shows a higher current intensity for CAF at 30 s. The NIC response between 0 and 30 s remained relatively constant, decreasing with time increase. This behavior indicates an equilibrium condition between adsorption and desorption of the analytes within 30 s. Thus, the time of 30 s and the pH value of 6.3 were chosen for the further studies.

The parameters of the DPV were studied, and the optimal conditions were evaluated considering the $W_{1/2}$ and the intensity of the analytical signals. More intense signals with good resolution were obtained with 90 mV modulation amplitude, 7.5 ms modulation time, and at a scan rate of 40 mV s⁻¹. The optimized values, along with the investigated intervals, are described in Table 2. Current graphs as a function of modulation amplitude, modulation time, and scan rate are available in Figure S4 (SI section).

Analytical performance of the method

From the optimization of parameters for NIC and CAF determination (Figure 6a), calibration curves were constructed for both analytes (Figure 6b). These analytical curves were generated by simultaneously adding the analytes, resulting in a linear dynamic range between 21.89 and 393.7 $\mu\text{mol L}^{-1}$ for NIC (Figure 6c) with a linear regression equation $I_p (\mu\text{A}) = -3.4 \times 10^{-8} + 8.56 \times 10^{-3} C_{\text{NIC}} (\mu\text{mol L}^{-1})$; LOD and LOQ were equal to 6.26 and 20.8 $\mu\text{mol L}^{-1}$, respectively,

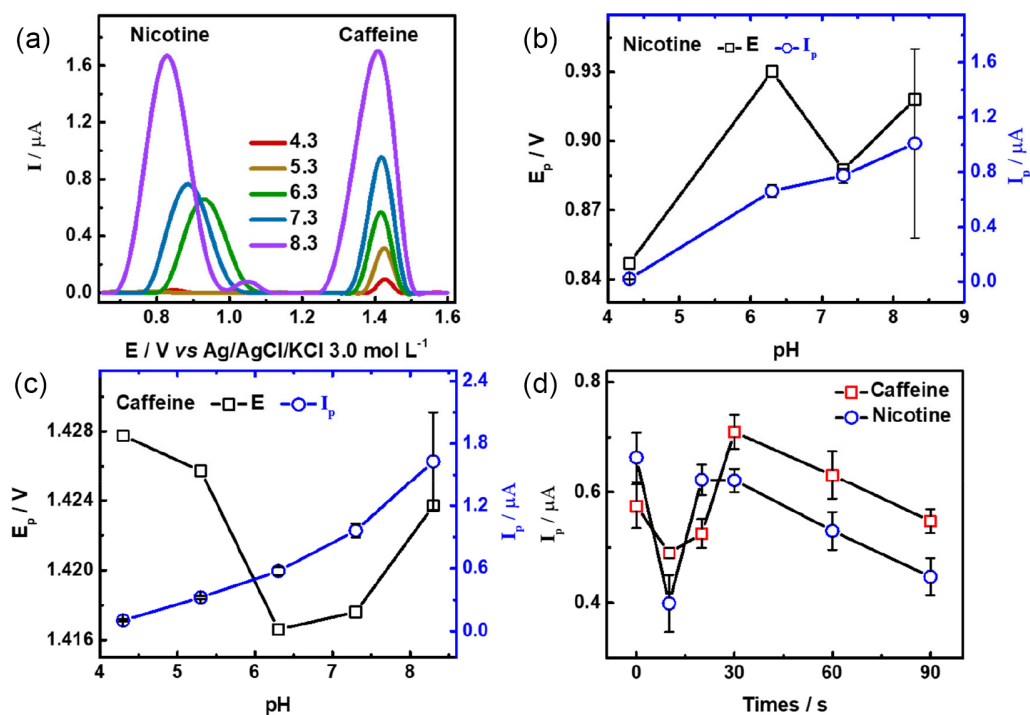


Figure 5. (a) DPV obtained in the presence of NIC ($196.0 \mu\text{mol L}^{-1}$) and CAF ($15.0 \mu\text{mol L}^{-1}$) under different pH conditions (4.3; 5.3; 6.3; 7.3; 8.3) of the 0.05 mol L^{-1} solution of 2HEAA; correlation between I_p and E_p of (b) NIC; and (c) CAF as a function of electrolyte pH; (d) relationship between the evaluated pre-concentration times (0 to 90 s) and I_p of NIC and CAF with 0.05 mol L^{-1} solution of 2HEAA (pH 6.3).

Table 2. Optimized experimental conditions for simultaneous determination of nicotine and caffeine in the presence of 2HEAA

Parameter	Range	Optimal conditions
Concentration of 2HEAA / (mol L ⁻¹)	0.01-0.20	0.05
pH	4.3-8.3	6.3
Pre-concentration time / s	0-90	30
Modulation amplitude / mV	30-120	90
Modulation time / ms	2.5-20.0	7.5
Scan rate / (mV s ⁻¹)	10-75	40

2HEAA: 2-hydroxyethylammonium acetate.

with $R^2 = 0.995$. Similarly, for CAF (Figure 6d), the linear range extended from 4.97 to 34.4 $\mu\text{mol L}^{-1}$, with the equation $I_p (\mu\text{A}) = 7.98 \cdot 10^{-8} + 4.90 \times 10^{-2} C_{\text{CAF}} (\mu\text{mol L}^{-1})$, resulting in a LOD of 0.82 $\mu\text{mol L}^{-1}$ and LOQ of 2.73 $\mu\text{mol L}^{-1}$, with $R^2 = 0.993$.

The figures of merit obtained in this study, using an unmodified glassy carbon electrode, and employing an alternative supporting electrolyte (2HEEA), are summarized in Table 3 and compared with the literature findings concerning the individual and simultaneous determination of NIC and CAF. The data indicate that the method developed with unmodified GCE in alternative electrolyte (2HEEA 0.05 mol L⁻¹) achieved satisfactory

analytical performance. Notably, LOD is comparable to those achieved for GCEs modified with various materials aimed at enhancing detectability, despite their associated costs.^{27-29,37} However, for NIC, the calculated LOD is approximately 6 times higher than those reported in the literature cited in Table 3, indicating lower detectability of this analyte in the developed system. Nevertheless, these values fall within the concentration range detected in different environments for NIC and CAF.^{38,39} For NIC, the levels found in wastewater ranged from 15.0 to 32,000.0 ng L⁻¹ in samples from different countries,³⁸ in physiological fluids (urine, sweat and saliva) concentrations were found between 150.0-2,498.0 ng per patch²⁷ and in breast milk there is possibility of contamination of up to 114.0 mg L⁻¹ (in smoking mothers).⁴⁰ For CAF, up to 1,500.0 ng L⁻¹ in freshwater ecosystems,³⁹ urine samples⁴¹ from people consuming at least two caffeine-containing beverages were found to be between 2.5 and 34.23 $\mu\text{g mL}^{-1}$ and in breast milk⁴² 12.0 to 179.0 ng mL⁻¹.

The method assessed in this study, utilizing 2HEEA as an alternative electrolyte underwent tests for accuracy, repeatability and reproducibility of the electrochemical signals of NIC and CAF. The results are summarized in Table S3 (SI section). The relative standard deviation (RSD) values obtained were all less than 10%. Specifically, for NIC, the RSD was 6.79 and 7.07%, respectively, whereas for CAF was 5.82 and 6.22%.

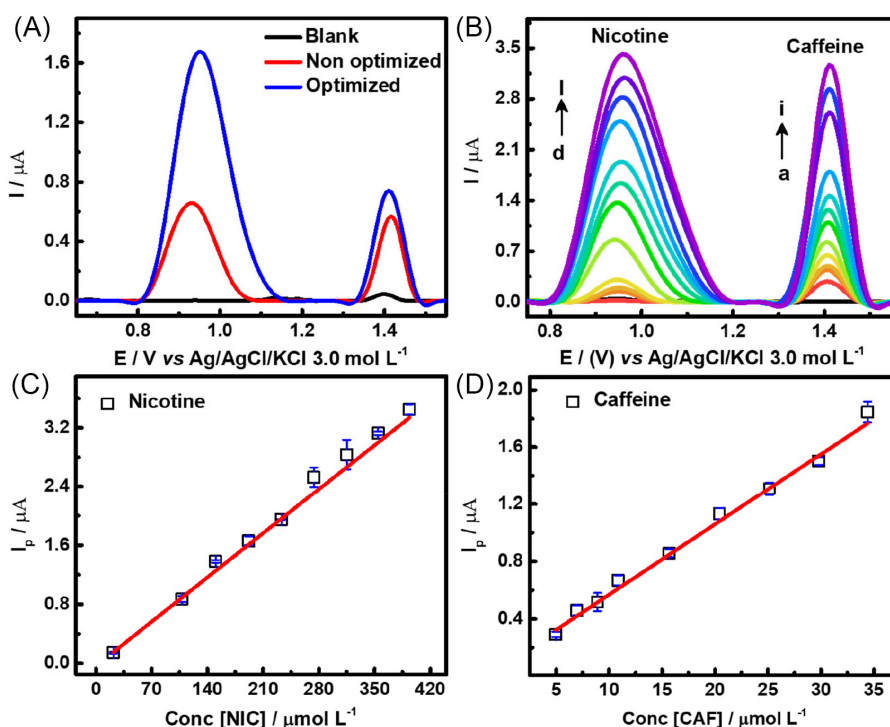


Figure 6. (A) DPV obtained in the 2HEEA electrolyte (0.05 mol L⁻¹, pH 6.3) in the presence of nicotine (196 $\mu\text{mol L}^{-1}$) and caffeine (15.0 $\mu\text{mol L}^{-1}$). Under non-optimized (red) and optimized (blue) analysis conditions; (B) DPV obtained under optimal conditions in the presence of different concentrations of caffeine (a = 4.97 to i = 34.42 $\mu\text{mol L}^{-1}$) and nicotine (d = 21.89 to l = 393.74 $\mu\text{mol L}^{-1}$). Linear correlation between anodic peak currents (I_p) and concentrations of (C) nicotine; and (D) caffeine.

Table 3. Comparison between merit figures of modified electrodes for nicotine and caffeine determination with the method developed using only the electrode without modification

Electrode	Analyte	LDR / ($\mu\text{mol L}^{-1}$)	LOD / ($\mu\text{mol L}^{-1}$)	Electrolyte	Reference
ESPE	NIC	1.0-375.0	0.6	PBS, pH 7.4	27
Poly(7A4HN2SA)/GCE	CAF	10.0-500.0	0.23	B-R, pH 2.0	28
Fe-MgNi ₂ O ₃ /GCE	NIC	50.0-6.000.0	0.098	PBS, pH 7.0	29
	CAF	50.0-4.000.0	0.276		
HA-GN-MWCNT/GCE	NIC	0.3-179.5	0.21	PBS, pH 7.0	37
	CAF	4.0-205.0	1.42		
	NIC+CAF	2.3-169.3	1.19 / 0.94		
poly(PRO)-MWCNT/GCE	CAF	10.04-93.26	21.99	PBS, pH 3.0	36
GCE	NIC	21.89-393.74	6.26	2HEAA, pH 6.3	this work
	CAF	4.97-34.42	0.82		

LDR: linear dynamic range; LOD: limit of detection; ESPE: silk-screened carbon electrode; Poly(7A4HN2SA): 7-amino-4-hydroxynaphthalene-2-sulfonic acid; Fe-MgNi₂O₃: pure iron(II)-doped MgNi₂O₃ nanoparticles; HA-GN-MWCNT: multi-walled hydroxyapatite-graphene-carbon nanotube ternary nanocomposite; poli(PRO)-MWCNT: electropolymerization of the proline-multiple walled carbon nanotubes; GCE: glassy carbon electrode; PBS: phosphate buffer; B-R: Britton-Robinson buffer; NIC: nicotine; CAF: caffeine; 2HEAA: 2-hydroxyethylammonium acetate.

The selectivity of the method was assessed for the analytes in the presence of both inorganic (CaCl₂, NaCl, KCl, NH₄Cl, MgCl₂ and Na₂SO₄) and organic (urea, ascorbic acid, sucrose, and glucose) species. The species comprised one or more complex samples utilized in this study for NIC and CAF recovery (Table 4). Figure 7 illustrates the percentage of interference of the species in the current-response intensity of the analytes. The results for the selectivity of the method demonstrated a relative standard deviation of less than 10% in the concentration levels of the investigated species. Regarding organic species, the interference in the signal-response of the analytes remained within the established limit of 10% in several studies.²⁶⁻²⁸ However, exceptions were noted for urea at level 2, ascorbic acid and sucrose at level 1 for NIC (Figure 7b) which exhibited values below than 15%. In the case of caffeine (Figure 7a), only ascorbic acid at level 2 displayed interference close to 20%. This observed behavior can be attributed to the competition among organic species for electroactive sites on the electrode, given that interferents are also electroactive species.⁴³⁻⁴⁵

Application of the method in sample analysis

The method was employed for the quantification of NIC and CAF in samples of river water, synthetic urine and commercial milk, all fortified with known concentrations of the analytes. The milk sample was considered due to its similar composition to breast milk. Some studies^{36,40} show that the consumption of CAF and NIC during pregnancy and breastfeeding can affect the health, temperament and short- and long-term development of children. In addition to affecting the response to hypoxic conditions, which is believed to be related to sudden infant death syndrome

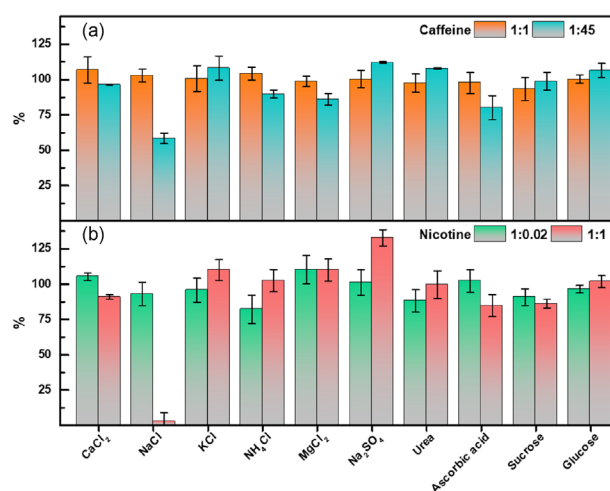


Figure 7. Variation in the analytical signal of (a) caffeine ($3.05 \mu\text{mol L}^{-1}$); and (b) nicotine ($138.3 \mu\text{mol L}^{-1}$) in the presence of organic and inorganic substances at levels 1 (1.0:1.0) and 2 (1.0:0.02 and 1.0:45) analyte:concomitant.

(SIDS).³⁷ In Figure 8a, the voltammograms obtained from the standard addition are presented, whereas in Figures 8b-8c, the curves for the first recovery of NIC and CAF in the milk sample are depicted. For the remaining samples (river water and urine), corresponding curves can be found in the SI section (Figure S5 to S10). The recovery values obtained varied within the range of 87.25 to 111.4% as detailed in Table 4, thus underscoring the selectivity of the method for the analytes in samples from various matrices.

In comparison with other reported studies utilizing buffer solution as supporting electrolyte and various modified electrodes, the system investigated in this study, employing the protic ionic liquid 2HEAA as a supporting electrolyte, demonstrated efficiency in determining and quantifying CAF and NIC analytes across different

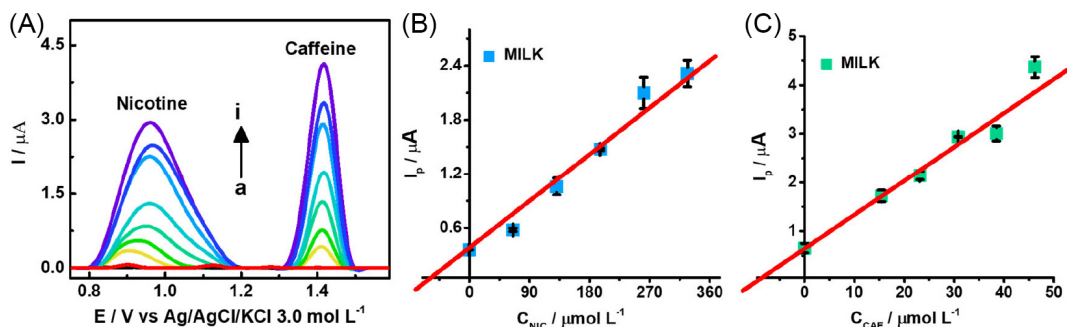


Figure 8. (A) DPV obtained in the presence of NIC and CAF in a commercial milk sample at NIC concentrations. Recovery curve for the first concentration level of (B) nicotine; and (C) caffeine.

Table 4. NIC and CAF recovery values in river water, synthetic urine, and milk samples (n = 3)

Sample	Analyte	[C] _{add} / (μmol L ⁻¹)	[C] _{Rec} / (μmol L ⁻¹)	Recovery / %
River water	nicotine	63.51	55.41	87.25 ± 0.85
		79.30	70.92	89.43 ± 0.64
	caffeine	3.04	3.39	111.40 ± 2.81
		4.56	4.58	100.45 ± 0.63
Synthetic urine	nicotine	6.08	6.04	99.42 ± 0.89
		126.51	115.46	91.26 ± 2.91
	caffeine	157.82	143.62	91.00 ± 5.32
		1.52	1.65	108.25 ± 2.65
Commercial milk	nicotine	3.04	2.95	96.80 ± 2.50
		4.56	4.61	101.05 ± 3.51
	caffeine	65.31	62.54	95.76 ± 0.29
		7.72	7.86	101.79 ± 7.44
		23.14	20.69	89.44 ± 0.65

[C]_{add}: added concentration; [C]_{Rec}: concentration recovered.

matrices. Coupled with the favorable properties exhibited by 2HEAA, including low toxicity, high conductivity, thermal and electrochemical stability (Table 1), the alternative electrolyte investigated holds promise for application as an electrolytic medium for redox processes, in the monitoring of various contaminants.

Conclusions

The investigation into the application of the protic ionic liquid as a supporting electrolyte for CAF and NIC determination demonstrated good performance. EIS analyses revealed that interfacial processes are significantly facilitated in the presence of 2HEAA, exhibiting a R_{CT} seven times lower than of the KCl solution. The percentage deviations for the repeatability and reproducibility measures were below 7.0%, indicating the high accuracy of the method. Moreover, the recovery levels of the analytes in the analyzed samples were satisfactory, ranging between 89.44 and 111.40% for caffeine and between 87.25 and 95.76% for nicotine.

Utilizing PIL as alternative electrolytes can offer a broad working range for monitoring contaminants that cannot be investigated with conventional electrolytes.

Acknowledgments

The authors gratefully acknowledge financial support from the Brazilian development agencies CNPq and CAPES and FAPITEC. We also extend our appreciation to the Corrosion and Nanotechnology Laboratory-LCNT, the Sergipe Oil and Gas Competence Center-NUPEG/PETROBRAS/UFS, the Multiuser Chemistry Laboratory Center-CLQM and to the Graduate Program in Chemistry (PPGQ) of the Federal University of Sergipe for the infrastructure support. Additionally, we thank the Nucleus of Renewable Energies and Energy Efficiency of Sergipe (NEREES) at the Sergipe Technological Park (SergipeTec) and the Institute of Technology and Research of the Tiradentes University - ITP/UNIT for their assistance with analyses.

Supplementary Information

Supplementary information is available free of charge at <http://jbcs.sbq.org.br> as PDF file.

Author Contributions

José Fernando de Macedo was responsible for conceptualization, data curation, formal analysis, investigation, methodology, validation, visualization, writing original draft; Jonatas O. Souza Silva for data curation, formal analysis, visualization, writing original draft; José Felipe dos Santos for data curation, formal analysis, visualization, writing original draft; José Carlos dos Santos Júnior for methodology, visualization, writing original draft; Micael S. Matos for formal analysis, investigation, visualization; Eliana M. Sussuchi for conceptualization, funding acquisition, methodology, project administration, resources, supervision, validation, visualization, writing original draft, review and editing.

References

- Jerzyński, T.; Stimson, G. V.; *Drugs, Habits and Social Policy* **2023**, *24*, 91. [Crossref]
- Coffee Consumption Worldwide from 2012/13 to 2021/22 with a Forecast to 2022/23 (in million 60 kg bags), <https://www.statista.com/statistics/292595/global-coffee-consumption/> accessed in July 2024.
- He, Z.; Xu, Y.; Rao, Z.; Zhang, Z.; Zhou, J.; Zhou, T.; Wang, H.; *Sci. Total Environ.* **2024**, *912*, 169604. [Crossref]
- Fiani, B.; Zhu, L.; Musch, B. L.; Briceno, S.; Andel, R.; Sadeq, N.; Ansari, A. Z.; *Cureus* **2021**, *13*, e15032. [Crossref]
- Nesil, T.; Kanit, L.; Pogun, S.; *Pharmacol., Biochem. Behav.* **2015**, *138*, 156. [Crossref]
- Li, J.; Wang, H.; Chen, H.; Li, X.; Liu, Y.; Hou, H.; Hu, Q.; *Food Chem. Toxicol.* **2024**, *185*, 114431. [Crossref]
- Everson, C. A.; Szabo, A.; Plyer, C.; Hammeke, T. A.; Stemper, B. D.; Budde, M. D.; *Exp. Neurol.* **2024**, *372*, 114620. [Crossref]
- Rohweder, R.; Schmalfluss, T. O.; Borniger, D. S.; Ferreira, C. Z.; Zanardini, M. K.; Lopes, G. P. T. F.; Barbosa, C. P.; Moreira, T. D.; Schuler-Faccini, L.; Sanseverino, M. T. V.; da Silva, A. A.; Abeche, A. M.; Vianna, F. S. L.; Fraga, L. R.; *Reprod. Toxicol.* **2024**, *123*, 108518. [Crossref]
- Lisowska, A.; Kasiak, P.; Rząca, M.; *Clin. Nutr. ESPEN* **2023**, *57*, 151. [Crossref]
- European Food Safety Authority (EFSA); *EFSA J.* **2015**, *13*, 4102. [Crossref]
- European Food Safety Authority (EFSA); *EFSA J.* **2023**, *21*, e08372. [Crossref]
- Oropesa, A. L.; Floro, A. M.; Palma, P.; *Environ. Sci. Pollut. Res.* **2017**, *24*, 16605. [Crossref]
- Dobaradaran, S.; Telgheder, U.; De-la-Torre, G. E.; Rockel, S. P.; Mutke, X. A. M.; Schmidt, T. C.; *Environ. Pollut.* **2024**, *341*, 122943. [Crossref]
- Picone, M.; Distefano, G. G.; Marchetto, D.; Russo, M.; Baccichet, M.; Brusò, L.; Zangrando, R.; Gambaro, A.; Volpi Ghirardini, A.; *Mar. Environ. Res.* **2022**, *181*, 105761. [Crossref]
- Szymczycha, B.; Borecka, M.; Białk-Bielińska, A.; Siedlewicz, G.; Pazdro, K.; *Sci. Total Environ.* **2020**, *713*, 136522. [Crossref]
- Silva, J. O. S.; Sant'Anna, M. V. S.; Gevaerd, A.; Lima, J. B. S.; Monteiro, M. D. S.; Carvalho, S. W. M. M.; Midori Sussuchi, E.; *Electroanalysis* **2021**, *33*, 2152. [Crossref]
- dos Santos, J. F.; Silva, J. O. S.; Macedo, J. F.; Júnior, J. C. S.; Almeida, W. S.; Midori Sussuchi, E. M.; *Electroanalysis* **2023**, *35*, e202200563. [Crossref]
- de Macedo, J. F.; Alves, A. A. C.; Sant'Anna, M. V. S.; Cunha, F. G. C.; Oliveira, G. A. R.; Lião, L. M.; Sussuchi, E. M.; *J. Appl. Electrochem.* **2022**, *52*, 729. [Crossref]
- Thakur, A.; Kumar, A.; *Results Eng.* **2023**, *20*, 101533. [Crossref]
- e Souza, G. A. L.; di Pietro, M. E.; Castiglione, F.; Martinez, P. F. M.; Fraenza, C. C.; Stallworth, P.; Greenbaum, S.; Triolo, A.; Battista Appetecchi, G.; Mele, A.; *Electrochim. Acta* **2024**, *474*, 143466. [Crossref]
- Mirzaei-Saatlo, M.; Asghari, E.; Shekaari, H.; Pollet, B.G.; Vinodh, R.; *Electrochim. Acta* **2024**, *474*, 143499. [Crossref]
- Li, F.; Mocchi, F.; Zhang, X.; Ji, X.; Laaksonen, A.; *Chin. J. Chem. Eng.* **2021**, *31*, 75. [Crossref]
- Ahmadpour, S.; Tashkhourian, J.; Hemmateenejad, B.; *J. Electroanal. Chem.* **2020**, *871*, 114296. [Crossref]
- Stettner, T.; Balducci, A.; *Energy Storage Mater.* **2021**, *40*, 402. [Crossref]
- Koukouvelis, D.; Pontillo, A. R. N.; Koutsoukos, S.; Pavlatou, E.; Detsi, A.; *J. Mol. Liq.* **2020**, *306*, 112929. [Crossref]
- Silva, J. O. S.; dos Santos, J. F.; Granja, H. S.; Almeida, W. S.; Loeser, T. F. L.; Freitas, L. S.; Bergamini, M. F.; Marcolino-Junior, L. H.; Sussuchi, E. M.; *Chemosphere* **2024**, *347*, 140707. [Crossref]
- Mehmeti, E.; Kilic, T.; Laur, C.; Carrara, S.; *Microchem. J.* **2020**, *158*, 105155. [Crossref]
- Geto, A.; Brett, C. M. A.; *Food Anal. Methods* **2021**, *14*, 2386. [Crossref]
- Reddy, S. L.; Arul, C.; Zhaoqi, L.; Lavanya, N.; Sekar, C.; *J. Electroanal. Chem.* **2020**, *878*, 114648. [Crossref]
- Suffredini, H. B.; Santos, M. C.; de Souza, D.; Codognoto, L.; Homem-de-Mello, P.; Honório, K. M.; da Silva, A. B. F.; Machado, S. A. S.; Avaca, L. A.; *Anal. Lett.* **2005**, *38*, 1587. [Crossref]
- Radhi, M. M.; Alasady, M. A. A.; Jabir, M. S.; *Port. Electrochim. Acta* **2020**, *38*, 139. [Crossref]
- Stočes, M.; Švancara, I.; *Electroanalysis* **2014**, *26*, 2655. [Crossref]

33. Belding, S. R.; Limon-Petersen, J. G.; Dickinson, E. J. F.; Compton, R. G.; *Angew. Chem.* **2010**, *122*, 9428. [Crossref]
34. Brett, C. M. A.; Brett, A. M. O.; *Electrochemistry: Principles, Methods, and Applications*, vol. 1, 1st ed.; Oxford University Press: New York, 1993.
35. Enache, T. A.; Chiorcea-Paquim, A.-M.; Fatibello-Filho, O.; Oliveira-Brett, A. M.; *Electrochem. Commun.* **2009**, *11*, 1342. [Crossref]
36. Aschemacher, N. A.; Gegenschatz, S. A.; Teglia, C. M.; Siano, Á. S.; Gutierrez, F. A.; Goicoechea, H. C.; *Talanta* **2024**, *267*, 125246. [Crossref]
37. Sudhan, N.; Lavanya, N.; Leonardi, S. G.; Neri, G.; Sekar, C.; *Sensors* **2019**, *19*, 3437. [Crossref]
38. Verovšek, T.; Heath, D.; Heath, E.; *Trends Environ. Anal. Chem.* **2022**, *34*, e00164. [Crossref]
39. Vieira, L. R.; Soares, A. M. V. M.; Freitas, R.; *Chemosphere* **2022**, *286*, 131675. [Crossref]
40. Aresta, A.; Palmisano, F.; Zambonin, C.; *Food Chem.* **2005**, *93*, 177. [Crossref]
41. Alzeer, S.; Odeh, A.; *Toxicologie Analytique et Clinique* **2022**, *34*, S90. [Crossref]
42. López-García, E.; Mastroianni, N.; Postigo, C.; Valcárcel, Y.; González-Alonso, S.; Barceló, D.; López de Alda, M.; *Food Chem.* **2018**, *245*, 159. [Crossref]
43. Zhuang, N.; Ma, J.; Yang, L.; Xue, R.; Qian, X.; Chen, M.; Zhang, S.; Chu, Z.; Dong, W.; Zhou, J.; Jiang, M.; *Microchem. J.* **2021**, *164*, 106075. [Crossref]
44. Naik, T. S. S. K.; Singh, S.; Narasimhappa, P.; Varshney, R.; Singh, J.; Khan, N. A.; Zahmatkesh, S.; Ramamurthy, P. C.; Shehata, N.; Kiran, G. N.; Sunil, K.; *Sci. Rep.* **2023**, *13*, 19995. [Crossref]
45. Mahale, R. S.; Vasanth, S.; Chikkegouda, S. P.; Rajendrachari, S.; Narsimhachary, D.; Basavegowda, N.; *Metals* **2023**, *13*, 1430. [Crossref]

Submitted: April 14, 2024

Published online: July 26, 2024